

# Temporally Propagated Masks and Bounding Boxes: Combining the Best of Both Worlds for Multi-Object Tracking

Tomasz Stanczyk

Inria centre at Université Côte d’Azur  
2004 Rte des Lucioles, 06902 Valbonne, France  
tomasz.stanczyk@inria.fr

Francois Bremond

Inria centre at Université Côte d’Azur  
2004 Rte des Lucioles, 06902 Valbonne, France  
francois.bremond@inria.fr

## Abstract

*Multi-object tracking (MOT) involves identifying and consistently tracking objects across video sequences. Traditional tracking-by-detection methods, while effective, often require extensive tuning and lack generalizability. On the other hand, segmentation mask-based methods are more generic but struggle with tracking management, making them unsuitable for MOT. We propose a novel approach, McByte, which incorporates a temporally propagated segmentation mask as a strong association cue within a tracking-by-detection framework. By combining bounding box and propagated mask information, McByte enhances robustness and generalizability without per-sequence tuning. Evaluated on four benchmark datasets - DanceTrack, MOT17, SoccerNet-tracking 2022, and KITTI-tracking - McByte demonstrates performance gain in all cases examined. At the same time, it outperforms existing mask-based methods. Implementation code will be provided upon acceptance.*

## 1. Introduction

Multi-object tracking (MOT) is a computer vision task that involves tracking objects (e.g., people) across video frames while maintaining consistent object IDs. MOT detects objects in each frame and associates them across consecutive frames. Applications include surveillance, automated behavior analysis (e.g., in hospitals), and autonomous driving, making reliable MOT trackers essential.

Tracking-by-detection methods [4, 12, 27, 35, 36, 40] use bounding boxes to detect objects in each frame and associate them with those from previous frames, based on cues like position, appearance, and motion. The resulting matches form “tracklets” over consecutive frames. However, these methods often require extensive hyper-parameter tuning for each dataset or even per single sequence, reducing their generalizability and limiting their application

across different datasets.

Segmentation mask-based methods [7, 29] generate masks to cover objects and track them across video frames. Trained on large datasets, these methods aim to capture the semantics of image patches, making them more generic. However, they are not designed for MOT, lacking robust management for tracking multiple entities and struggling to detect new objects entering the scene. Additionally, they rely entirely on mask predictions for object positioning, which can be problematic when the predictions are noisy or inaccurate.

In this paper, we explore using a temporally propagated segmentation mask as an association cue to assess its effectiveness in MOT. We propose a novel tracking-by-detection method that combines mask propagation and bounding boxes to improve the association between tracklets and detections. The mask propagation is managed according to the tracklet lifespan, while the mask is used in a controlled manner to enhance tracking performance. Since the temporal mask propagation model is trained on a large dataset, it makes the entire tracking process more generic. Unlike existing tracking-by-detection methods, our approach does not require tuning hyperparameters for each video sequence.

Tracking multiple objects at once often involves handling challenging occlusions, where only a small part of the subject might be visible, e.g. a leg of a person. Temporally propagated mask can be especially helpful in such cases, when the visible shape can considerably differ from the subject. A visual example is presented in Fig. 1.

We note explicitly that incorporating temporally propagated mask, which also involves temporal coherency, is different than using a static mask coming directly from an image segmentation model (such as SAM [20]) independently per each frame. We detail it in Sec. 3.2. To the best of our knowledge, using the mask temporal propagation within the problem of MOT has not been done before.

Our work covers specifically the problem of MOT, where we associate newly detected bounding boxes with previ-

ously tracked bounding boxes. Other challenges, such as Single Object Tracking (SOT), Video Object Segmentation (VOS), or Multi-Object Tracking and Segmentation (MOTS), although relevant, necessitate further modeling and are beyond the scope of this paper. In our work, we measure specifically the performance of bounding box association. For the mask performance, we refer the reader to the related works of temporal propagation models [6, 8].

We evaluate our incorporation of the temporally propagated mask as an association cue against a baseline tracker, showing clear benefits for MOT. Our tracker is tested on four diverse MOT datasets, achieving the highest performance from tracking-by-detection algorithms on Dance-Track [33], MOT17 [28], SoccerNet-tracking 2022 [9] and KITTI-tracking [16]. These results highlight the advantages of using mask propagation, eliminating the need for per-sequence hyper-parameter tuning.

Our contribution in this work is summarized as follows:

1. We provide an evaluation of the existing mask-based approaches in the MOT domain, demonstrating their unsuitability (Sec. 4.5).
2. We propose a novel approach adapting a temporally propagated object segmentation mask as a strong and powerful cue, which, contrarily to a static mask, is incorporated into MOT for the first time. We describe the approach in Sec. 3.3.
3. We design an MOT tracking algorithm substantiating the idea and incorporating the temporally propagated mask as an association cue between tracklets and detections, detailed in Secs. 3.1 and 3.2. The tracker overcomes the limitations of mask-based approaches by performing proper tracklet management and including other important association cues as well as the limitations of the baseline tracking-by-detection approaches, by making the tracking process more robust and generic.
4. We evaluate and discuss the use of the temporally propagated mask as an association cue with different conditions within a tracking-by-detection algorithm in the ablation study (Sec. 4.3). Further, we evaluate our tracker incorporating the mask cue on four different datasets (in Sec. 4.4), comparing it to state-of-the-art tracking-by-detection approaches and demonstrating performance gain thanks to the attentive mask propagation usage, while not tuning per-sequence parameters.

## 2. Related Work

Different types of algorithms for tracking multiple objects at the same time have been developed in the community. We provide a brief overview of the existing methods related to our work.



Figure 1. Temporally propagated mask can be helpful in cases of high occlusion. The person with the red mask is tracked only by its limited visible parts (pointed by yellow arrows for the clarity). Input image data from [28]. Best seen in color.

### 2.1. Transformer-based and other types of method

Transformer-based methods [13, 14, 38, 41] use attention mechanisms to learn tracking trajectories and object associations from training data, following an end-to-end approach. These methods perform well on video sequences where subjects remain mostly on the scene, such as Dance-Track [33], but struggle with sequences where subjects frequently enter and exit, like in the MOT17 dataset [28], despite being designed for MOT. For this reason, we do not directly compare our method with transformer-based approaches in the main paper, though their results are listed together with the other approaches and ours in Appendix B.

Other types of MOT methods have also been proposed in the community, such as global optimization (offline) methods [5] or joint detection and tracking methods [37, 39]. Analogously to the transformer-based methods, they are not directly comparable and we list them for reference in Appendix B.

### 2.2. Tracking-by-detection methods

The tracking-by-detection approach detects objects in each video frame and associates them into tracklets, linking the same objects across frames.

ByteTrack [40] is a powerful tracking-by-detection algorithm that uses the YOLOX [15] detector, associating tracklets based on the intersection over union (IoU) between bounding boxes of tracklets and new detections. It provides strong tracklet management and serves as a solid baseline for MOT. Several works have built on ByteTrack. OC-SORT [4] enhances state estimation by computing virtual trajectories during occlusion. StrongSORT [12] adds re-identification (re-ID) features as cues, camera motion compensation, and NSA Kalman filter [11]. C-BIoU [35] extends the association process by buffering (enlarging) bounding boxes, while HybridSORT [36] adds cues like confidence modeling and height-modulated IoU alongside existing strong cues.

Although these algorithms perform well on popular MOT datasets, they are highly sensitive to parameters. ByteTrack, for instance, explicitly tunes parameters like

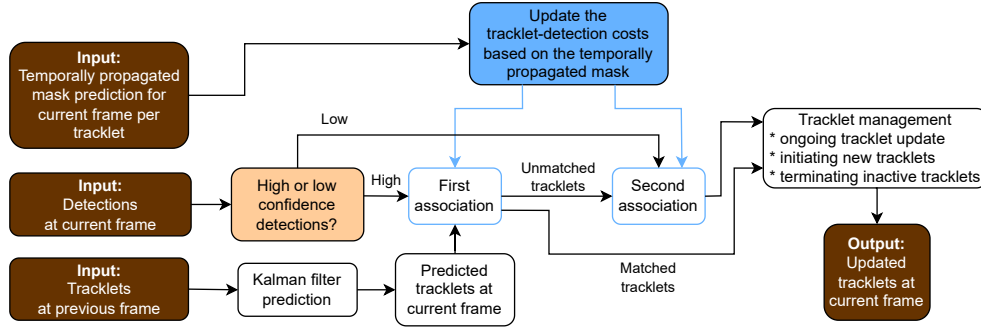


Figure 2. McByte tracking pipeline with the mask cue guidance. Temporally propagated mask signal is incorporated as an association cue in the tracklet-detection association steps.

high-confidence detection thresholds per test sequence, as noted on its GitHub page<sup>1</sup> and in the code<sup>2</sup>, which affects the tracking performance. Extensions of ByteTrack [4, 12, 27, 36], sharing the same code also rely on per-sequence parameter tuning. This tuning process is costly and impractical for larger datasets like DanceTrack [33], SoccerNet-tracking [9], and KITTI-tracking [16], as well as for generalizing across datasets. In contrast, our method, incorporating the temporally propagated segmentation mask as an association cue, avoids per-sequence tuning, making it more robust and generic, as we further demonstrate in Sec. 4.4.

### 2.3. Segmentation mask models

**Mask creation.** The Segment-Anything Model (SAM) [20] is a highly effective image segmentation model trained on a massive dataset, delivering impressive segmentation outputs. Recently, SAM 2 [29] was introduced, enhancing SAM’s performance and enabling video-level segmentation across entire sequences. However, once tracking starts, SAM 2 cannot track new objects, limiting its use in complete MOT tasks. Later in this section, we discuss a SAM 2-based bounding box tracker combined with Grounding Dino [24] (see: *Mask-based tracking systems*).

**Mask temporal propagation.** XMem [6] is a mask temporal propagation model for video object segmentation (VOS), based on the Atkinson-Shiffrin Memory Model [1], enabling long-term tracking of segmentation masks. Its successor, Cutie [8], improves segmentation by incorporating object encoding from mask memory and better distinguishing the object from the background. Note that image segmentation models like SAM [20] only constitute the creation of the initial mask at the designated frames. Mask temporal propagation models then aim to infer the referred mask over the next frames in a video sequence.

While generally powerful in their target domains, both XMem and Cutie are not directly suitable for MOT as they do not involve bounding boxes and might provide inaccurate mask predictions as listed in their performance on video object segmentation [6, 8]. Therefore, we propose a novel MOT algorithm that combines temporally propagated masks with bounding boxes, improving tracking performance. Our ablation studies in Sec. 4.3 show that using the mask in a controlled manner, and along with other MOT mechanisms, is more effective than relying solely on the mask signal.

**Mask-based tracking systems.** Segmentation mask models have already been used to build tracking systems. DEVA [7], which enhances XMem [6], proposes decoupled video segmentation and bi-directional propagation, and builds a tracking system with boxes and masks. However, MOT requires a robust tracklet management and an occlusion handling system, which is not available within DEVA.

Grounded SAM 2<sup>3</sup> is a tracking system combining Grounding Dino [24] and SAM 2 [29] for video object segmentation, designed to track bounding boxes and maintain object IDs. However, SAM 2’s inability to add new objects once tracking begins makes it unsuitable for MOT. It tracks objects in segments, but merging those segments is not always successful.

MASA [22] is a mask feature-based adapter [3, 18] trained with SAM [20], offering inference modes for video segmentation and object tracking. In tracking, MASA provides features for matching object detections across frames. However, it struggles with longer occlusions and missing or incorrect detections. While MASA has been tested on a few MOT datasets [22], the mentioned limitations weaken its performance and reduce its generalizability across varied datasets.

Existing mask-based tracking algorithms, though trained

<sup>1</sup><https://github.com/ifzhang/ByteTrack>, see: Test on MOT17.

<sup>2</sup>[https://github.com/ifzhang/ByteTrack/blob/main/yolox/evaluators/mot\\_evaluator.py](https://github.com/ifzhang/ByteTrack/blob/main/yolox/evaluators/mot_evaluator.py), lines 146-157 (at the moment of submitting this paper)

<sup>3</sup>Method not officially published, yet with implementation code available: <https://github.com/IDEA-Research/Grounded-SAM-2>

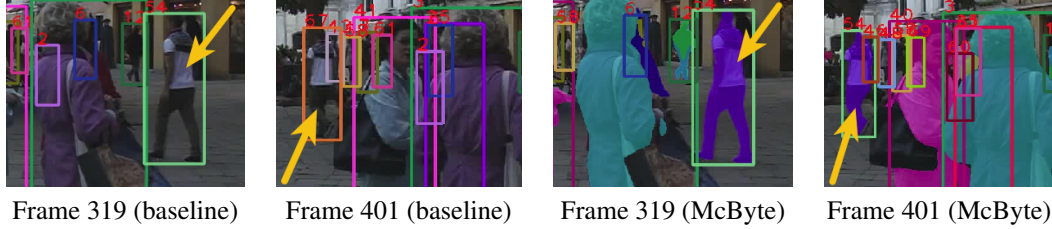


Figure 3. Visual output comparison between the baseline and McByte. With the temporally propagated mask guidance, McByte can handle longer occlusion in the crowd - see the subject with ID 54 on the output of McByte. Input image data from [28]. Best seen in color.

on large datasets for extracting semantic features, fail to handle challenges like occlusion and track initiation. We discuss it more in detail in Sec. 4.5, where we show that their performance on MOT tasks is significantly lower than other methods. Our proposed MOT tracker incorporates the temporally propagated mask as an association cue while leveraging powerful mechanisms like tracklet management and additional cues (e.g., bounding box position, motion). As we demonstrate in Sec. 4.5, our approach performs considerably better than existing mask-based systems, even when they are adapted to MOT format and evaluation.

### 3. Proposed method

#### 3.1. Preliminaries

Multi-object tracking (MOT) involves tracking detected objects across video frames by forming tracklets that link detections over consecutive frames. In tracking-by-detection methods [4, 12, 27, 35, 36, 40], existing tracklets from previous frames are associated with new detections in the current frame. This process uses association cues such as object position and motion to build a cost matrix representing potential tracklet-detection matches. The association problem considered as the bipartite matching problem is then solved using the Hungarian algorithm [21], which matches tracklets with detections to extend them while minimizing total cost. Pairs with costs above the pre-defined matching threshold are excluded.

In our baseline, ByteTrack [40], new detections are split into high and low confidence groups, handled separately in the association process. The baseline uses intersection over union (IoU) as the primary association metric. Tracklet positions are predicted using a Kalman Filter [19] and compared to detection bounding boxes using IoU scores. Cost matrix entries are filled with  $1 - \text{IoU}$  for each tracklet-detection pair. Further, tracklet management includes initiating, updating, and terminating tracklets. For more details, we refer the reader to the ByteTrack paper [40].

In our work, we study a temporally propagated segmentation mask as a powerful association cue for MOT. We extend the baseline algorithm [40] and combine the mask information with bounding box information to create

our novel **masked-cued** algorithm, which we call McByte. Fig. 2 shows the overview of our tracking pipeline pointing to where the temporally propagated mask is involved as an association cue. We note that we consider the problem of MOT, where we perform and evaluate the association between the bounding boxes of detections and tracklets.

In the next sections, we describe the creation and handling of the mask within our MOT tracking algorithm (Sec. 3.2) and our regulated use of the temporally propagated mask as an association cue (Sec. 3.3).

#### 3.2. Mask creation and handling

Since the temporally propagated mask as a cue has to facilitate associating a tracklet with the correct detection, it must be well correlated with the tracklets and handled accordingly. This process is originally not straightforward and thus we design the following approach of mask handling to synchronise it with the processed tracklets.

During tracking in McByte, each tracklet gets its own mask, which is then temporally propagated across frames to update the mask predictions. At first, we use an image segmentation model to create a segmentation mask for each new tracklet. It is performed only for a newly appeared object and to initialize a new mask.

Separately, during the next frames, a temporal propagator is used to infer the updated mask positions, while aiming to keep the spatio-temporal consistency of the mask. The propagator predictions are analyzed and used in the tracklet-detection association process, as detailed in Sec. 3.3. We manage the temporally propagated masks in sync with the tracklet management system, creating new masks for new tracklets and removing them when a tracklet is terminated.

We provide more detailed information and a diagram including both mask creation and mask temporal propagation in Appendix E.

#### 3.3. Regulated use of the mask

A temporally propagated (TP) segmentation mask can be a strong association cue if used correctly. However, mask predictions from the temporal propagator might sometimes be incorrect, as seen in related works [6, 8] and thus unreliable, making it essential to regulate the mask’s use as a



cue.

In the association process, we update the cost matrix entries using the TP mask, particularly in cases of ambiguity, where a tracklet could match multiple detections or vice versa. Ambiguity often arises from IoU-based matches when tracked objects are close, causing significant overlap in bounding boxes and similar IoU scores. If IoU is below the matching threshold for more than one tracklet-detection pair, we treat it as ambiguity.

For each potential ambiguous tracklet-detection match, we apply a strategy consisting of the following conditions.

1. We check if the considered tracklet’s TP mask is actually visible on the scene. Subjects can be entirely occluded resulting in no mask prediction at the current frame.
2. We check if the TP mask prediction is confident enough, i.e. if the average mask probability for the given object from the mask propagator is above the set mask confidence threshold.

Further, we compute two key ratios between the TP mask and detection bounding box:

- the bounding box coverage of the mask, referred to as mask match no. 1,  $mm_1$ :

$$mm_1^{i,j} = \frac{|pix(mask(tracklet_i)) \cap pix(bbox_j)|}{|pix(mask(tracklet_i))|} \quad (1)$$

- the mask fill ratio of the bounding box, referred to as mask match no. 2,  $mm_2$ :

$$mm_2^{i,j} = \frac{|pix(mask(tracklet_i)) \cap pix(bbox_j)|}{|pix(bbox_j)|} \quad (2)$$

where  $pix(\cdot)$  denotes pixels of the mask or within the bounding box, and  $mask(\cdot)$  denotes the TP mask assigned to the tracklet.  $|\cdot|$  denotes the cardinality of the set. Note that all  $mm_1, mm_2 \in [0, 1]$ . In Fig. 4, we show how  $mm_1$  and  $mm_2$  can vary depending on the TP mask and bounding box position. We discuss it more in detail in Appendix E. Going further with the conditions:

3. We check if the mask fill ratio of the bounding box  $mm_2$  occupies a significant portion of the bounding box.
4. We check if the bounding box coverage of the mask  $mm_1$  is sufficiently high.

Only if all these conditions hold, we update the tracklet-detection association in the cost matrix using the following formula:

$$costs^{i,j} = costs^{i,j} - mm_2^{i,j} \quad (3)$$

where  $costs^{i,j}$  denotes the cost between tracklet  $i$  and detection  $j$ . With this fusion of the available information, we consider both modalities, TP masks and bounding boxes to enhance the association process. The updated cost matrix, enriched by the mask signal, is passed to the Hungarian matching algorithm to find optimal tracklet-detection pairs.

Following conditions 1-4. ensures that the TP mask cue is controlled, and the cost matrix is updated only when the mask is reliable. The impact of each condition, along with

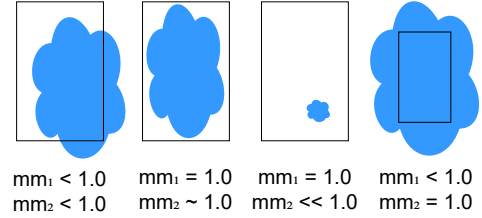


Figure 4. Cases showing the differences in  $mm_1$  and  $mm_2$  (Sec. 3.3) values of a temporally propagated mask (in blue) within a bounding box. The most optimal case for the mask to provide a good guidance is the second one from the left, where both  $mm_1$  and  $mm_2$  are as close to 1 as possible.

the absence of any, is demonstrated in the ablation study (Sec. 4.3, Tab. 1). Further details on these conditions are included in Appendix E.

Further, using  $mm_1$  directly to influence the cost matrix could be misleading, as multiple TP masks could fully fit within the same bounding box, all resulting in  $mm_1 = 1.0$ . Therefore, we use  $mm_1$  only as a gating condition and  $mm_2$  to influence the cost matrix.

Our baseline is optimized for bounding boxes, so we retain the use of the Hungarian matching algorithm over the cost matrix, but we carefully incorporate the TP mask signal to enhance the association process. In the ablation study (Sec. 4.3), we show that combining bounding boxes with the mask is more effective than using the mask alone, and demonstrate the advantages of incorporating the TP mask signal as an additional association cue over a purely bounding box-based approach.

In Fig. 3, we show that McByte can handle challenging scenarios such as long-term occlusion in crowd due to the TP mask signal in the controlled manner as an association cue. More visual examples are available in Appendix E.

### 3.4. Handling camera motion

When the camera moves, tracklet and detection bounding boxes may become less accurate due to object motion and blurring. To address this, we integrate camera motion compensation (CMC) into our process (which fuses temporally propagated mask and bounding box information) to enhance the accuracy of bounding box estimates. This approach follows existing methods [12, 27]. More details on CMC are provided in Appendix E. The final McByte version includes CMC, and its impact is shown in the ablation study in Sec. 4.3, Tab. 1.

## 4. Experiments and discussion

### 4.1. Implementation details

For object detections, we follow the practices of our baseline [40] and use the YOLOX [15] detector pretrained on

the relevant dataset, unless stated otherwise. As in baseline, detections are divided into high and low confidence sets based on a defined threshold. However, on the contrary to the baseline which considers different values per video sequence, we always use the same threshold for all sequences. We fix it as 0.6, which is the default value of our baseline, i.e. when the baseline is evaluated on datasets without tuning per sequence.

For mask creation, we use SAM [20], ensuring fair comparison with related works, with the vit\_b model and weights from SAM’s authors. As a mask temporal propagator, we use Cutie [8] with the weights provided by the authors, Cutie base mega. Note that we use the image segmentation model (SAM) only to create and initialize the masks for the newly appeared objects at the scene. For the association cue between the tracklets and detections we process the propagated mask from the mask temporal propagator (Cutie). All experiments are conducted on an Nvidia A100 GPU with 40 GB of memory.

## 4.2. Datasets and evaluation metrics

We evaluate McByte on four person tracking datasets with diverse characteristics, to demonstrate the generalizability of our method. We present results on DanceTrack [33], MOT17 [28], SoccerNet-tracking 2022 [9], and KITTI-tracking [16], while using detection sources per dataset as per community practices for fair comparison.

DanceTrack [33] features people performing dances with highly non-linear motion and subtle camera movements, while the number of individuals stays mostly constant. We use YOLOX pre-trained on DanceTrack for detections, following our baseline [40].

MOT17 [28] involves tracking people in public spaces under varying conditions, such as lighting, pedestrian density, and camera stability. We use YOLOX pre-trained on MOT17 for detections as provided by the the baseline [40].

SoccerNet-tracking 2022 [9] contains soccer match videos, where players move rapidly and look alike in the same team. Camera movement is always present and oracle detections are provided by the dataset authors.

KITTI-tracking [16] captures scenes from car view, with varied pedestrian density and frequent camera movement. It also considers another class, car, which can help to assess the generalizability of the tracking method. Following community practices [4, 12], we use PermaTr [34] detections.

We report three standard MOT metrics: HOTA [26], IDF1 [31] and MOTA [2], focusing on HOTA and IDF1 for evaluating the tracking performance. IDF1 measures the tracking quality and identity preservation, while HOTA includes association, detection and localization. MOTA primarily measures detection quality and we report it for the result completeness. Higher values in these metrics indicate better performance.

Method	HOTA	IDF1	MOTA
baseline [40]: no mask	47.1	51.9	88.2
a1: either mask or no assoc.	48.6	44.4	80.8
a2: either mask or IoU for assoc.	45.3	41.5	82.2
a3: IoU and mask if ambiguity	56.6	57.0	89.5
a4: a3 + mask confidence	57.3	57.7	89.6
a5: a4 + $mm_2$	58.8	60.1	89.6
a6: a5 + $mm_1$	62.1	63.4	89.7
McByte: a6 + cmc	<b>62.3</b>	<b>64.0</b>	<b>89.8</b>

Table 1. Ablation study on DanceTrack [33] validation set listing the effects of the imposed constraints on using the temporally propagated mask as an association cue.

Method	HOTA	IDF1	MOTA
Baseline, DanceTrack val	47.1	51.9	88.2
McByte, DanceTrack val	<b>62.3</b>	<b>64.0</b>	<b>89.8</b>
Baseline, SoccerNet-tracking 2022 test	72.1	75.3	94.5
McByte, SoccerNet-tracking 2022 test	<b>85.0</b>	<b>79.9</b>	<b>96.8</b>
Baseline, MOT17 val	68.4	80.2	78.2
McByte, MOT17 val	<b>69.9</b>	<b>82.8</b>	<b>78.5</b>
Baseline, KITTI-tracking test	54.3	-	63.7
McByte, KITTI-tracking test	<b>57.0</b>	-	<b>68.9</b>

Table 2. Ablation study comparing McByte with the baseline [40] on four different datasets. As SoccerNet-tracking 2022 [9] and KITTI-tracking [16] (pedestrian) do not contain validation set split, we report the results on the test sets. KITTI evaluation server does not provide IDF1 scores.

## 4.3. Ablation studies

We perform an ablation study to demonstrate the impact of incorporating the temporally propagated (TP) mask as an association cue along with the conditions discussed in Sec. 3.3. We evaluate the following variants:

- a1: Uses only the TP mask signal for association if the mask is visible for the given tracklet, without ambiguity checks (Sec. 3.3). The value of  $mm_2^{i,j}$  is directly assigned to  $costs^{i,j}$  in Eq. (3). No association occurs if there is no mask.
- a2: Similar to a1, but if the TP mask is unavailable, intersection over union (IoU) scores are used for association, as in the baseline [40].
- a3: Adds an ambiguity check (Sec. 3.3). If the TP mask is visible, mask and bounding box information are fused as shown in Eq. (3). If no mask is available, IoU scores are used as in the baseline.
- a4: Builds on a3, incorporating the mask confidence check (condition 2 in Sec. 3.3).
- a5: Extends a4 by adding the  $mm_2$  value check from condition 3 in Sec. 3.3.
- a6: Further extends a5 with the  $mm_1$  value check from

Method	HOTA	IDF1	MOTA
ByteTrack [40]	47.7	53.9	89.6
OC-SORT [4]	55.1	54.9	92.2
Deep OC-SORT [27]	61.3	61.5	92.3
C-BIoU [35] *	45.8	52.0	88.4
StrongSORT++ [12]	55.6	55.2	91.1
Hybrid-SORT [36]	65.7	67.4	91.8
McByte (ours)	<b>67.1</b>	<b>68.1</b>	<b>92.9</b>

Table 3. Comparing McByte with state-of-the-art tracking-by-detection algorithms on DanceTrack test set [33].

Method	HOTA	IDF1	MOTA
With parameter tuning per sequence			
ByteTrack [40]	63.1	77.3	80.3
StrongSORT++ [12]	64.4	79.5	79.6
OC-SORT [4]	63.2	77.5	78.0
Deep OC-SORT [27]	64.9	80.6	79.4
Hybrid-SORT [36]	64.0	78.7	79.9
Without parameter tuning per sequence			
ByteTrack [5]	62.8	77.1	78.9
C-BIoU [35] *	62.4	77.1	79.5
McByte (ours)	<b>64.2</b>	<b>79.4</b>	<b>80.2</b>

Table 4. Comparing McByte with state-of-the-art tracking-by-detection algorithms on MOT17 test set [28].

Method	HOTA	IDF1	MOTA
ByteTrack [40]	72.1	75.3	94.5
OC-SORT [4]	82.0	76.3	<b>98.3</b>
C-BIoU [35] *	72.7	76.4	95.4
McByte (ours)	<b>85.0</b>	<b>79.9</b>	96.8

Table 5. Comparing McByte with state-of-the-art tracking-by-detection algorithms on SoccerNet-tracking 2022 test set [9].

Method	HOTA	MOTA	HOTA	MOTA
	Pedestrian		Car	
ByteTrack [40]	54.3	63.7	47.3	34.9
PermaTr [34]	47.4	65.1	78.0	91.3
OC-SORT [4]	54.7	65.1	76.5	90.3
StrongSORT++ [12]	54.5	67.4	77.8	90.4
McByte (ours)	<b>57.0</b>	<b>68.9</b>	<b>80.8</b>	<b>92.5</b>

Table 6. Comparing McByte with state-of-the-art tracking-by-detection algorithms on KITTI-tracking test set [16]. KITTI evaluation server does not provide IDF1 scores.

condition 4 in Sec. 3.3.

The results of each variant are listed in Tab. 1. In variant a1, where only the TP mask signal is used for association, we can see that despite HOTA increase, IDF1 decreases with respect to the baseline. It is caused by the fact that the

mask use is uncontrolled and chaotic. With TP mask possibly providing incorrect results, the association cues can be misleading. If we perform the association either based only on TP mask or only on IoU (depending on the availability of the mask), as in variant a2, we might face an inconsistency of the cues between tracklets and detections from the same frame and the next frames. This might lead to performance degradation. However, when we use properly both cues fusing the available information (variant a3), we can observe significant performance gain. We explain it as the algorithm is initially designed to work on bounding boxes while TP mask is a valuable guiding cue which can improve existing association mechanisms. When the mask signal is the only cue or not properly fused with the IoU cue, a lower performance might be obtained (as in a1 and a2).

Adding the conditional check based on TP mask confidence (variant a4) further improves the performance, because sometimes mask might be uncertain or incorrect providing misleading association guidance. Adding the minimal  $mm_2$  value check (variant a5) also provides performance gain, because this check filters out the tracklet TP masks which could be considered as a noise or tiny parts of people almost entirely occluded. Another performance gain can be observed with the minimal  $mm_1$  value check (variant a6). This check determines if the TP mask of the tracked person is actually within the bounding box and not too much outside it. Since the detection box might not be perfect, we allow small parts of the tracklet mask to be outside the bounding box, but its major part must be within the bounding box, so that the TP mask can be used for guiding the association between the considered tracklet-detection pair. As it is shown, it further helps. Finally, we add the camera motion compensation (CMC), denoted as McByte in Tab. 1, which also provides some performance gain.

We compare our McByte tracking algorithm to the baseline [40] across the four datasets, as shown in Tab. 2. Performance improvements are seen in all cases, though the gains vary by dataset due to different characteristics. For example, DanceTrack [33] features non-linear motion, where the TP mask signal is particularly helpful in tracking occluded subjects, whereas IoU might struggle. In SoccerNet-tracking 2022 [9], where occlusions are fewer but motion is more abrupt (e.g., players running), the mask aids in successfully capturing players, despite similar outfits among team members.

The performance gain on MOT17 [28] is smaller than on the previous datasets due to crowded scenes and smaller, distant people, making it harder for the TP mask to capture them accurately. The quality of detections, especially for small or uncertain bounding boxes, makes it difficult for the mask to comply with our conditions ( $mm_1$  and  $mm_2$ ), which rely on bounding boxes. KITTI-tracking shows a similar trend yet with higher gain, with less distant pedes-

trians and different quality of detections. Although gains vary by dataset, McByte consistently improves performance (Tab. 2), demonstrating its robustness and general applicability. TP mask incorporated as an association cue helps to handle challenging scene situations such as high occlusions and reduced subject visibility as shown in Fig. 1.

MyByte also performs better than the baseline when the public detections are given. Due to the space limits, we show it in Appendix D.

#### 4.4. Comparison with state of the art tracking-by-detection methods

We compare McByte with state-of-the-art tracking-by-detection algorithms across the test sets of the four diversified datasets. The results, listed in Tabs. 3 to 6 show that McByte achieves the highest HOTA, IDF1 and MOTA scores on DanceTrack [33] (Tab. 3), MOT17 [28] (Tab. 4) and KITTI-tracking [16] (Tab. 6). In case of SoccerNet-tracking 2022 [9] (Tab. 5), McByte achieves the highest HOTA and IDF1 scores, and the second highest MOTA score.

The KITTI-tracking test server evaluates both pedestrian and car classes. We also test ByteTrack [40], our baseline, with the same detection set for comparison. ByteTrack performs poorly on the car class because its parameters are specifically set for tracking people. When using PermaTr [34] detections, which include cars, ByteTrack struggles to generalize, leading to lower performance, though it performs comparably on the pedestrian class. Our method performs well on pedestrians, but also on other objects, such as cars, which we demonstrate in Tab. 6.

On the MOT17 [28] test set, unlike the baseline [40] and derived methods [4, 12, 27, 36], we do not tune parameters per sequence. We aim at developing a generalizable tracker without the need for changes on different sequences or datasets. We reach the best scores among the non-tuned trackers. We use the result of ByteTrack [40] not being tuned per sequence as reported in [5]. Juxtaposed with the methods which do tune their parameters per sequence, we achieve improvements over the baseline [40] and comparable performance with other methods.

Additionally, C-BIoU [35] is marked with an asterisk in Tabs. 3 to 5. As no implementation is published, and not all necessary details for reproduction are provided, we reproduce the method based on the available descriptions and report the best results we have obtained. We describe it more in detail in Appendix C.

#### 4.5. Comparison with other methods using mask

We evaluate existing mask-based tracking methods: DEVA [7], Grounded SAM 2 [24, 29] and MASA [22] on the MOT17 validation set. Each method is tested with its original settings and with YOLOX [15] trained on

Method	HOTA	IDF1	MOTA
DEVA, original settings	31.8	31.3	-89.4
DEVA, with YOLOX	24.7	20.4	-239.7
Grounded SAM 2, original settings	43.4	47.6	18.4
Grounded SAM 2, with YOLOX	47.5	54.1	43.0
MASA, original settings	45.5	53.6	36.9
MASA, with YOLOX	63.5	73.6	74.0
McByte (ours)	<b>69.9</b>	<b>82.8</b>	<b>78.5</b>

Table 7. Comparison with the other tracking methods using segmentation mask: DEVA [7], Grounded SAM 2 [20, 24] and MASA [22] on MOT17 validation set [28].

MOT17 [28] from our baseline [40], as used in McByte. Results in Tab. 7 show that all methods perform significantly worse than McByte.

DEVA [7] lacks a tracklet management system, leading to chaotic tracklet handling, resulting in negative MOTA scores, which occur when errors exceed the number of objects [10]. Adding YOLOX detections worsens the performance by introducing more redundant and noisy tracklets and masks.

Grounded SAM 2 [24, 29] struggles with segment-based tracking, where merging segments into full tracklets is unreliable. Though YOLOX detections improve the performance, the results remain far below McByte’s performance.

MASA [22] fails to handle longer occlusions and misses many detections in its original setup, yielding low MOT performance. While YOLOX detections improve its results, it still lags behind McByte and even the baseline due to ongoing challenges with occlusions and missed detections.

These results highlight that existing mask-based methods are unsuitable for MOT. In contrast, McByte effectively combines temporally propagated mask-based association with bounding box processing and tracklet management, making it better suited for MOT tasks.

More results and details on DEVA, Grounded SAM 2, and MASA experiments are available in Appendix A.

## 5. Conclusion

In this paper, we explore the use of a temporally propagated segmentation mask as an association cue for MOT. We develop a new mechanism that incorporates the mask propagation into a tracking-by-detection approach, fusing temporally propagated mask and bounding box information to improve bounding box-based multi-object tracking performance. Results from four datasets show the effectiveness of this approach, with our algorithm boosting MOT performance. Additionally, it outperforms other systems that rely primarily on segmentation masks, highlighting that when carefully managed, the mask can serve as a powerful association cue for MOT.



## Acknowledgement

This work was granted access to the HPC resources of IDRIS under the allocation 2024-AD011014370 made by GENCI. The work was performed within the 3IA Côte d’Azur funding.

## References

- [1] R.C. Atkinson and R.M. Shiffrin. Human memory: A proposed system and its control processes. pages 89–195. Academic Press, 1968. 3
- [2] Keni Bernardin and Rainer Stiefelhausen. Evaluating multiple object tracking performance: The clear mot metrics. *EURASIP Journal on Image and Video Processing*, 2008, 2008. 6
- [3] Deblina Bhattacharjee, Sabine Süssstrunk, and Mathieu Salzmann. Vision transformer adapters for generalizable multi-task learning, 2023. 3
- [4] Jinkun Cao, Jiangmiao Pang, Xinshuo Weng, Rawal Khirrodgar, and Kris Kitani. Observation-centric sort: Rethinking sort for robust multi-object tracking. In *Proceedings of the IEEE/CVF Conference on Computer Vision and Pattern Recognition (CVPR)*, pages 9686–9696, 2023. 1, 2, 3, 4, 6, 7, 8, 13
- [5] Orcun Cetintas, Guillem Brasó, and Laura Leal-Taixé. Unifying short and long-term tracking with graph hierarchies. In *Proceedings of the IEEE/CVF Conference on Computer Vision and Pattern Recognition (CVPR)*, pages 22877–22887, 2023. 2, 7, 8, 12, 13
- [6] Ho Kei Cheng and Alexander G. Schwing. XMem: Long-term video object segmentation with an atkinson-shiffrin memory model. In *Proceedings of the European Conference on Computer Vision (ECCV)*, 2022. 2, 3, 4, 15, 16
- [7] Ho Kei Cheng, Seoung Wug Oh, Brian Price, Alexander Schwing, and Joon-Young Lee. Tracking anything with decoupled video segmentation. In *Proceedings of the IEEE/CVF International Conference on Computer Vision (ICCV)*, 2023. 1, 3, 8, 11, 12
- [8] Ho Kei Cheng, Seoung Wug Oh, Brian Price, Joon-Young Lee, and Alexander Schwing. Putting the object back into video object segmentation. In *Proceedings of the IEEE/CVF Conference on Computer Vision and Pattern Recognition (CVPR)*, 2024. 2, 3, 4, 6, 15, 16
- [9] Anthony Cioppa, Silvio Giancola, Adrien Deliege, Le Kang, Xin Zhou, Zhiyu Cheng, Bernard Ghanem, and Marc Van Droogenbroeck. Soccernet-tracking: Multiple object tracking dataset and benchmark in soccer videos. In *Proceedings of the IEEE/CVF Conference on Computer Vision and Pattern Recognition*, pages 3491–3502, 2022. 2, 3, 6, 7, 8, 14
- [10] Patrick Dendorfer, Aljossa Ossep, Anton Milan, Daniel Cremers, Ian Reid, Stefan Roth, and Laura Leal-Taixe. Motchallenge: A benchmark for single-camera multiple target tracking. *International Journal of Computer Vision*, 129:1–37, 2021. 8, 11, 14
- [11] Yunhao Du, Junfeng Wan, Yanyun Zhao, Binyu Zhang, Zhihang Tong, and Junhao Dong. Giaotracker: A comprehensive framework for mcmot with global information and optimizing strategies in visdrone 2021. In *Proceedings of the IEEE/CVF International Conference on Computer Vision (ICCV) Workshops*, pages 2809–2819, 2021. 2
- [12] Yunhao Du, Zhicheng Zhao, Yang Song, Yanyun Zhao, Fei Su, Tao Gong, and Hongying Meng. Strongsort: Make deepsort great again. *IEEE Transactions on Multimedia*, 2023. 1, 2, 3, 4, 5, 6, 7, 8, 13, 17
- [13] Ruopeng Gao and Limin Wang. MeMOTR: Long-term memory-augmented transformer for multi-object tracking. In *Proceedings of the IEEE/CVF International Conference on Computer Vision (ICCV)*, pages 9901–9910, 2023. 2, 13
- [14] Ruopeng Gao, Yijun Zhang, and Limin Wang. Multiple object tracking as id prediction, 2024. 2, 13
- [15] Zheng Ge, Songtao Liu, Feng Wang, Zeming Li, and Jian Sun. YOLOX: Exceeding yolo series in 2021. *arXiv preprint arXiv:2107.08430*, 2021. 2, 5, 8, 11, 14, 15
- [16] Andreas Geiger, Philip Lenz, and Raquel Urtasun. Are we ready for autonomous driving? the kitti vision benchmark suite. In *Conference on Computer Vision and Pattern Recognition (CVPR)*, 2012. 2, 3, 6, 7, 8, 14
- [17] Kaiming He, Xiangyu Zhang, Shaoqing Ren, and Jian Sun. Deep Residual Learning for Image Recognition. In *Proceedings of 2016 IEEE Conference on Computer Vision and Pattern Recognition*, pages 770–778. IEEE, 2016. 11
- [18] Neil Houlsby, Andrei Giurgiu, Stanislaw Jastrzebski, Bruna Morrone, Quentin De Laroussilhe, Andrea Gesmundo, Mona Attariyan, and Sylvain Gelly. Parameter-efficient transfer learning for NLP. In *Proceedings of the 36th International Conference on Machine Learning*, pages 2790–2799. PMLR, 2019. 3
- [19] R. E. Kalman. A New Approach to Linear Filtering and Prediction Problems. *Journal of Basic Engineering*, 82(1):35–45, 1960. 4, 17
- [20] Alexander Kirillov, Eric Mintun, Nikhila Ravi, Hanzi Mao, Chloe Rolland, Laura Gustafson, Tete Xiao, Spencer Whitehead, Alexander C. Berg, Wan-Yen Lo, Piotr Dollár, and Ross Girshick. Segment anything. *Proceedings of the IEEE/CVF International Conference on Computer Vision (ICCV)*, 2023. 1, 3, 6, 8, 12, 15
- [21] H. W. Kuhn. The hungarian method for the assignment problem. *Naval Research Logistics Quarterly*, 2(1-2):83–97, 1955. 4, 14
- [22] Siyuan Li, Lei Ke, Martin Danelljan, Luigi Piccinelli, Mattia Segu, Luc Van Gool, and Fisher Yu. Matching anything by segmenting anything. *CVPR*, 2024. 3, 8, 11, 12
- [23] Tsung-Yi Lin, Michael Maire, Serge J. Belongie, Lubomir D. Bourdev, Ross B. Girshick, James Hays, Pietro Perona, Deva Ramanan, Piotr Dollár, and C. Lawrence Zitnick. Microsoft coco: Common objects in context. *CoRR*, abs/1405.0312, 2014. 11
- [24] Shilong Liu, Zhaoyang Zeng, Tianhe Ren, Feng Li, Hao Zhang, Jie Yang, Chunyuan Li, Jianwei Yang, Hang Su, Jun Zhu, et al. Grounding dino: Marrying dino with grounded pre-training for open-set object detection. *arXiv preprint arXiv:2303.05499*, 2023. 3, 8, 11, 12
- [25] Ze Liu, Yutong Lin, Yue Cao, Han Hu, Yixuan Wei, Zheng Zhang, Stephen Lin, and Baining Guo. Swin transformer:

- Hierarchical vision transformer using shifted windows. In *Proceedings of the IEEE/CVF International Conference on Computer Vision (ICCV)*, 2021. 11
- [26] Jonathon Luiten, Aljosa Osep, Patrick Dendorfer, Philip Torr, Andreas Geiger, Laura Leal-Taixé, and Bastian Leibe. Hota: A higher order metric for evaluating multi-object tracking. *International Journal of Computer Vision*, pages 1–31, 2020. 6
- [27] Gerard Maggolino, Adnan Ahmad, Jinkun Cao, and Kris Kitani. Deep oc-sort: Multi-pedestrian tracking by adaptive re-identification. *arXiv preprint arXiv:2302.11813*, 2023. 1, 3, 4, 5, 7, 8, 13, 17
- [28] A. Milan, L. Leal-Taixé, I. Reid, S. Roth, and K. Schindler. MOT16: A benchmark for multi-object tracking. *arXiv:1603.00831 [cs]*, 2016. arXiv: 1603.00831. 2, 4, 6, 7, 8, 11, 12, 13, 14, 15, 17
- [29] Nikhila Ravi, Valentin Gabeur, Yuan-Ting Hu, Ronghang Hu, Chaitanya Ryali, Tengyu Ma, Haitham Khedr, Roman Rädle, Chloe Rolland, Laura Gustafson, Eric Mintun, Junting Pan, Kalyan Vasudev Alwala, Nicolas Carion, Chaoyuan Wu, Ross Girshick, Piotr Dollár, and Christoph Feichtenhofer. Sam 2: Segment anything in images and videos. *arXiv preprint arXiv:2408.00714*, 2024. 1, 3, 8, 11
- [30] Shaoqing Ren, Kaiming He, Ross B. Girshick, and Jian Sun. Faster r-cnn: Towards real-time object detection with region proposal networks. In *NIPS*, pages 91–99, 2015. 14
- [31] Ergys Ristani, Francesco Solera, Roger Zou, Rita Cucchiara, and Carlo Tomasi. Performance measures and a data set for multi-target, multi-camera tracking. In *Computer Vision – ECCV 2016 Workshops*, pages 17–35, Cham, 2016. Springer International Publishing. 6
- [32] Ethan Rublee, Vincent Rabaud, Kurt Konolige, and Gary Bradski. Orb: an efficient alternative to sift or surf. pages 2564–2571, 2011. 17
- [33] Peize Sun, Jinkun Cao, Yi Jiang, Zehuan Yuan, Song Bai, Kris Kitani, and Ping Luo. Dancetrack: Multi-object tracking in uniform appearance and diverse motion. *Proceedings of the IEEE/CVF Conference on Computer Vision and Pattern Recognition (CVPR)*, 2021. 2, 3, 6, 7, 8, 11, 12, 13, 14
- [34] Pavel Tokmakov, Jie Li, Wolfram Burgard, and Adrien Gaidon. Learning to track with object permanence. In *Proceedings of the IEEE/CVF International Conference on Computer Vision (ICCV)*, 2021. 6, 7, 8
- [35] Fan Yang, Shigeyuki Odashima, Shoichi Masui, and Shan Jiang. Hard to track objects with irregular motions and similar appearances? make it easier by buffering the matching space. In *Proceedings of the IEEE/CVF Winter Conference on Applications of Computer Vision (WACV)*, pages 4799–4808, 2023. 1, 2, 4, 7, 8, 13, 14
- [36] Mingzhan Yang, Guangxin Han, Bin Yan, Wenhua Zhang, Jinqing Qi, Huchuan Lu, and Dong Wang. Hybrid-sort: Weak cues matter for online multi-object tracking. In *Proceedings of the AAAI Conference on Artificial Intelligence*, pages 6504–6512, 2024. 1, 2, 3, 4, 7, 8, 13
- [37] En Yu, Zhuoling Li, Shoudong Han, and Hongwei Wang. Relationtrack: Relation-aware multiple object tracking with decoupled representation. *IEEE Transactions on Multimedia*, 25:2686–2697, 2022. 2, 13
- [38] Fangao Zeng, Bin Dong, Yuang Zhang, Tiancai Wang, Xiangyu Zhang, and Yichen Wei. Motr: End-to-end multiple-object tracking with transformer. In *European Conference on Computer Vision (ECCV)*, 2022. 2, 13
- [39] Yifu Zhang, Chunyu Wang, Xinggang Wang, Wenjun Zeng, and Wenyu Liu. Fairmot: On the fairness of detection and re-identification in multiple object tracking. *International Journal of Computer Vision*, 129:3069–3087, 2021. 2, 13
- [40] Yifu Zhang, Peize Sun, Yi Jiang, Dongdong Yu, Fucheng Weng, Zehuan Yuan, Ping Luo, Wenyu Liu, and Xinggang Wang. Bytetrack: Multi-object tracking by associating every detection box. 2022. 1, 2, 4, 5, 6, 7, 8, 11, 12, 13, 14, 15, 16
- [41] Yuang Zhang, Tiancai Wang, and Xiangyu Zhang. Motrv2: Bootstrapping end-to-end multi-object tracking by pre-trained object detectors. In *Proceedings of the IEEE/CVF Conference on Computer Vision and Pattern Recognition (CVPR)*, pages 22056–22065, 2023. 2, 13
- [42] Xingyi Zhou, Vladlen Koltun, and Philipp Krähenbühl. Tracking objects as points. *Proceedings of the European Conference on Computer Vision (ECCV)*, 2020. 13
- [43] Xingyi Zhou, Rohit Girdhar, Armand Joulin, Philipp Krähenbühl, and Ishan Misra. Detecting twenty-thousand classes using image-level supervision. In *Proceedings of the European Conference on Computer Vision (ECCV)*, 2022. 11

# Appendices

This supplementary material contains the following appendices as referred in the main paper:

- [A](#) More experiments and details with mask-based tracking systems
- [B](#) State-of-the-art comparison with transformer-based and other types of method
- [C](#) More information on C-BIoU
  - [C.1](#) Our C-BIoU implementation and its performance
  - [C.2](#) C-BIoU with temporally propagated mask as an association cue
- [D](#) McByte and baseline on public detections
- [E](#) McByte components more in detail
  - [E.1](#) Mask processing and management
  - [E.2](#) Tracklet mask visibility at the scene
  - [E.3](#) Mask confidence
  - [E.4](#) Bounding box coverage (mm1) and mask fill ratio (mm2)
  - [E.5](#) Camera motion compensation
  - [E.6](#) Additional visual example

## A. More experiments and details with mask-based tracking systems

We evaluate DEVA [7], Grounded SAM 2 [24, 29], and MASA [22] on MOT datasets, saving each bounding box output per frame in MOT format [10]. The limitations of these methods when applied to MOT are described in Secs. 2.3 and 4.5 of the main paper.

We conduct additional experiments to thoroughly explore the performance differences between the mask-based tracking systems and our McByte. These include several variants on the MOT17 [28] validation set, as well as a corresponding table for the DanceTrack [33] validation set, analogous to the one presented in the main paper.

Tab. 8 presents various experimental variants on the MOT17 validation set, where different detectors and parameters are used. The variants marked with ‡ correspond to those discussed in the main paper.

For DEVA, we first run the default settings using the Grounding Dino [24] detector with the "person" prompt and a confidence threshold of 0.35 to accept bounding boxes. Then, we replace it with the YOLOX [15] detector, trained on the MOT17 dataset from our baseline [40]. We test two threshold values, 0.6 and 0.7. In our baseline, initialization of the new tracklets happens for the values 0.1 higher than the high confidence detection threshold. As we consider the default value of 0.6 for the latter (Sec. 4.1 in the main paper), we also experiment with the value of 0.7 with DEVA and other mask based systems.

For Grounded SAM 2 [24, 29], we use the "Video Object Tracking with Continuous ID" version as specified on its

GitHub page<sup>4</sup>. Initially, we run it with the original settings, using the Grounding Dino [24] detector with the "person" prompt, a confidence detection threshold of 0.25, and a step value of 20. The step value defines how often detections are processed (e.g., every 20th frame) to create mask tracklets, functioning as the segment length (we refer to tracking objects in segments mentioned in the main paper, Sec. 2.3). We then test an analogous variant with a step value of 100.

Next, we integrate YOLOX detector with weights from our baseline [40] and run variants with step values of 20, 100, and 1 (thus processing detections every frame), using different bounding box allowance thresholds of 0.25, 0.6, and 0.7 (analogous to the DEVA experiments). We also attempt to run a variant with the segment length set to the entire video sequence, but it fails due to excessive GPU memory requirements. Additionally, this setup would only track objects visible in the first frame.

MASA [22] offers several models for inference. We test variants using two different feature backbones: GroundingDINO [24] (GDino) and ResNet-50 [17] (R50). For the GroundingDINO variant, we use the Detic-SwinB detector [25, 43] with the "person" prompt, applying the original detection confidence threshold of 0.2. We also run a similar variant with the YOLOX detector trained on the COCO [23] dataset, as provided by the authors, using a confidence threshold of 0.3 default for this variant.

Further, we incorporate the YOLOX detector with weights from our baseline [40] and test variants with detection confidence thresholds of 0.3, 0.6, and 0.7, analogously to DEVA and Grounded SAM 2. Additionally, we run the ResNet-50 feature variants with the YOLOX COCO model (threshold 0.3) and the baseline-pre-trained weights (thresholds 0.3, 0.6, 0.7).

As shown in Tab. 8, McByte outperforms the referenced mask-based systems, making it more suitable for MOT.

Tab. 9 presents the performance of DEVA, Grounded SAM 2, and MASA on the DanceTrack [33] validation set. The listed variants correspond to those marked with ‡ in Tab. 8 and are the ones reported in the main paper on MOT17.

On DanceTrack, McByte also demonstrates significantly higher performance, reinforcing its effectiveness and suitability for MOT.

## B. State-of-the-art comparison with transformer-based and other types of method

There exist MOT methods outside the tracking-by-detection domain manifesting performance differences, but usually these methods are not directly comparable, because they

<sup>4</sup><https://github.com/IDEA-Research/Grounded-SAM-2>

Details	HOTA	IDF1	MOTA
DEVA			
GDino "person", th. 0.35 ‡	<b>31.8</b>	<b>31.3</b>	<b>-89.4</b>
YOLOX ByteTrack, th. 0.6 ‡	24.7	20.4	-239.7
YOLOX ByteTrack, th. 0.7	27.0	23.7	-187.8
Grounded SAM 2			
GDino "person", th. 0.25, step 20 ‡	43.4	47.6	18.4
GDino "person", th. 0.25, step 100	44.0	49.0	15.5
YOLOX ByteTrack, th. 0.25, step 20	46.4	51.6	36.0
YOLOX ByteTrack, th. 0.6, step 20 ‡	<b>47.5</b>	54.1	43.0
YOLOX ByteTrack, th. 0.7, step 20	47.4	54.1	44.3
YOLOX ByteTrack, th. 0.25, step 100	46.8	54.2	30.2
YOLOX ByteTrack, th. 0.6, step 100	47.4	<b>54.9</b>	34.8
YOLOX ByteTrack, th. 0.7, step 100	47.4	<b>54.9</b>	35.9
YOLOX ByteTrack, th. 0.25, step 1	43.0	43.9	36.2
YOLOX ByteTrack, th. 0.6, step 1	44.4	46.5	44.9
YOLOX ByteTrack, th. 0.7, step 1	44.3	46.7	<b>46.5</b>
MASA			
GDino feat. Detic-SwinB "person", th 0.2	46.8	52.1	24.3
GDino feat. YOLOX COCO, th 0.3	45.4	53.1	36.9
GDino feat. YOLOX ByteTrack, th 0.3	61.8	70.8	71.3
GDino feat. YOLOX ByteTrack, th 0.6	63.4	73.3	73.8
GDino feat. YOLOX ByteTrack, th 0.7	62.5	71.9	72.9
R50 feat. YOLOX COCO, th 0.3 ‡	45.5	53.6	36.9
R50 feat. YOLOX ByteTrack, th 0.3	62.5	72.0	71.5
R50 feat. YOLOX ByteTrack, th 0.6 ‡	<b>63.5</b>	<b>73.6</b>	<b>74.0</b>
R50 feat. YOLOX ByteTrack, th 0.7	62.6	72.3	73.0
McByte			
McByte (ours)	<b>69.9</b>	<b>82.8</b>	<b>78.5</b>

Table 8. Extended comparison with the other tracking methods using segmentation mask: DEVA [7], Grounded SAM 2 [20, 24] and MASA [22] on MOT17 validation set [28], while changing their parameters. ‡ denotes the variants reported in the main paper and in Tab. 9.

Method	HOTA	IDF1	MOTA
DEVA, original settings	21.9	15.8	-347.1
DEVA, with YOLOX	20.1	13.3	-423.9
Grounded SAM 2, original settings	51.3	48.0	73.5
Grounded SAM 2, with YOLOX	52.9	49.6	81.6
MASA, original settings	38.2	34.9	71.9
MASA, with YOLOX	46.0	41.1	85.6
McByte (ours)	<b>62.3</b>	<b>64.0</b>	<b>89.8</b>

Table 9. Comparison with the other tracking methods using segmentation mask: DEVA [7], Grounded SAM 2 [20, 24] and MASA [22] on DanceTrack validation set [33]. The reported variants correspond to the variants with ‡ symbol in Tab. 8

make certain hypotheses, e.g. global optimization on the whole video. At the same time, these methods might perform visibly worse on some benchmarks as we discuss be-

low. On the contrary, we stress that McByte performs well on all the discussed benchmarks (Secs. 4.3 and 4.4 of the main paper). McByte is a tracking-by-detection approach, which is the main focus of our work. For an additional reference, though, we also list performance of the transformer-based, global optimization, and joint detection and tracking methods.

Tab. 10 shows extended state-of-the art comparison on MOT17 [28] test set. Note that analogously to the main paper, we also put the result of ByteTrack [40] not being tuned per sequence as reported in [5]. Transformer-based methods perform visibly lower than the tracking-by-detection methods (including ours) as they struggle with the subjects frequently entering and leaving the scene. In contrast, SUSHI [5], which is a powerful global optimization approach, reaches highly satisfying performance. However, it accesses all the video frames at same time while process-



Method	HOTA	IDF1	MOTA
Transformer-based			
MOTR [38]	57.8	68.6	73.4
MeMOTR [13]	58.8	71.5	72.8
MOTRv2 [41]	62.0	75.0	78.6
MOTIP [14]	59.2	71.2	75.5
Global optimization			
SUSHI [5]	66.5	83.1	81.1
Joint detection and tracking			
FairMOT [39]	59.3	72.3	73.7
RelationTrack [37]	61.0	75.8	75.6
CenterTrack [42]	52.2	64.7	67.8
Tracking-by-detection with parameter tuning per sequence			
ByteTrack [40]	63.1	77.3	80.3
StrongSORT++ [12]	64.4	79.5	79.6
OC-SORT [4]	63.2	77.5	78.0
Deep OC-SORT [27]	64.9	80.6	79.4
Hybrid-SORT [36]	64.0	78.7	79.9
Tracking-by-detection without parameter tuning per sequence			
ByteTrack [5]	62.8	77.1	78.9
C-BIoU [35] *	62.4	77.1	79.5
McByte (ours)	64.2	79.4	80.2

Table 10. Extended state-of-the-art method comparison on MOT17 [28] test set.

ing detections and associating the tracklets, which makes it impossible to run in online settings. This makes the performance not directly comparable and therefore, we do not include it in the main paper. Current state-of-the-art joint detection and tracking methods generally perform lower than the tracking-by-detection methods. In this paradigm, the detection and association step is performed jointly. In our method, we perform these two steps separately and focus on the association part.

Tab. 11 presents extended state-of-the-art comparison on DanceTrack [33] test set. As in this dataset the subjects remain mostly at the scene, the transformer-based methods performance is more satisfying. The performance of transformer-based methods can be both higher [14, 41] or lower [13, 38] compared to the tracking-by-detection methods. For similar reasons, the global optimization method, SUSHI [5] can also perform higher than the other tracking-by-detection methods on this dataset, or lower, e.g. when compared to our method. On this dataset, joint detection and tracking methods also manifest lower performance than the tracking-by-detection methods. As in the case of the MOT17 benchmark, the performance of the mentioned

Method	HOTA	IDF1	MOTA
Transformer-based			
MOTR [38]	54.2	51.5	79.7
MeMOTR [13]	63.4	65.5	85.4
MOTRv2 [41]	73.4	76.0	92.1
MOTIP [14]	67.5	72.2	90.3
Global optimization			
SUSHI [5]	63.3	63.4	88.7
Joint detection and tracking			
FairMOT [39]	39.7	40.8	82.2
CenterTrack [42]	41.8	35.7	86.8
Tracking-by-detection			
ByteTrack [40]	47.7	53.9	89.6
OC-SORT [4]	55.1	54.9	92.2
Deep OC-SORT [27]	61.3	61.5	92.3
C-BIoU [35] *	45.8	52.0	88.4
StrongSORT++ [12]	55.6	55.2	91.1
Hybrid-SORT [36]	65.7	67.4	91.8
McByte (ours)	67.1	68.1	92.9

Table 11. Extended state-of-the-art method comparison on DanceTrack [33] test set.

different method types is not directly comparable and thus not included in the main paper.

## C. More information on C-BIoU

### C.1. Our C-BIoU implementation and its performance

The C-BIoU [35] paper does not provide a public implementation or sufficient details for code reproduction. We implement C-BIoU based on the available information and report the best results on the datasets evaluated by the original algorithm. These results, marked with an asterisk, are shown in the main paper (Tabs. 3 to 5) and in Tabs. 10 to 12 of this supplementary material.

Based on the descriptions in the C-BIoU work [35], especially regarding tracklet management and tracklet-detection association, the core of the method strongly resembles ByteTrack [40]. Thus, we extend ByteTrack by incorporating cascaded buffered intersection over union [35] for the association process. Where C-BIoU does not specify parameters, we default to those used in ByteTrack. For the MOT17 test set, we do not tune detection confidence parameters per sequence (referred in Sec. 2.2 of the main paper) and apply a fixed 0.6 threshold for all sequences and datasets. This is the default value of ByteTrack, i.e. when ByteTrack is run on datasets without tuning per sequence. Regarding the two buffering scales in C-BIoU, we use the values 0.3 and 0.4, which were reported to result in the best

HOTA on the DanceTrack validation set in the C-BIoU paper [35]. Although we also test the values 0.3 and 0.5 (as mentioned in the framework figure from C-BIoU), the 0.3 and 0.4 combination performs slightly better in our experiments.

Additionally, following C-BIoU’s supplementary material, we adopt the most optimal *max\_age* values per dataset. The *max\_age* parameter defines the maximum lifespan (in frames) of a tracklet that has not been matched to a detection before it is terminated and removed. For DanceTrack [33], we set *max\_age* to 100, and for SoccerNet-tracking 2022 [9], we set it to 60. In case of MOT17 [28], where this value is not directly specified, we test three different *max\_age* values: 20, 60, and 100 (as listed in C-BIoU’s supplementary material). We select the value that results in the highest performance on the MOT17 validation set, which is 60, and then use this value for testing on the MOT17 test set to report the final results.

The results are presented in Tabs. 3 to 5 of the main paper. Compared to the baseline, ByteTrack [40], the improvement is modest (Tab. 5) or shows slight degradation (Tabs. 3 and 4). This could be due to tuning issues, as many parameters were not specified in the C-BIoU paper. Specifically, with buffered intersection over union (IoU), the association search space expands, leading to more potential associations and lower IoU-based distances. However, the matching thresholds for the linear association steps (using the Hungarian Algorithm [21]), which filter out unlikely matches, are not provided. Default thresholds from ByteTrack [40] may allow more matches, introducing unresolved ambiguities and potentially degrading performance.

We do not evaluate C-BIoU on KITTI-tracking test set, because the test evaluation server has a very limited number of submissions per person [16] (less than MOT17 test server [10, 28]). We use these submissions for McByte and our baseline [40]. Besides, the results on KITTI-tracking test set are not reported in the work of C-BIoU [35].

## C.2. C-BIoU with temporally propagated mask as an association cue

We also evaluate temporally propagated (TP) mask as an association cue within the C-BIoU [35] tracker to demonstrate the generalizability and advantage of our approach within MOT. We follow exactly the same steps as with incorporating the TP mask in our baseline [40] for McByte. Tab. 12 includes the performance comparison of the C-BIoU tracker with and without the TP mask as a cue. The results show that our TP mask-based approach is beneficial beyond single baseline and that it can improve MOT performance of other trackers as well.

As in the other result tables, the asterisk means that no official implementation is published and that we reproduce the C-BIoU method based on the available informa-

Method	HOTA	IDF1	MOTA
DanceTrack test set			
C-BIoU [35] *	45.8	52.0	88.4
C-BIoU [35] * with our TP mask cue	<b>67.6</b>	<b>70.2</b>	<b>92.4</b>
SoccerNet-tracking 2022 test set			
C-BIoU [35] *	72.7	76.4	95.4
C-BIoU [35] * with our TP mask cue	<b>84.6</b>	<b>79.0</b>	<b>98.2</b>

Table 12. Comparison of another tracking algorithm [35], with and without our approach of temporally propagated (TP) mask as an association cue (Appendix C.2).

tion, described in detail in Appendix C.1. MOT17 [28] and KITTI-tracking [16] test evaluation servers allow limited submissions which we use for McByte and our baseline [40]. Therefore, we report the results of this study on DanceTrack [33] and SoccerNet-tracking 2022 [9] test sets.

## D. McByte and baseline on public detections

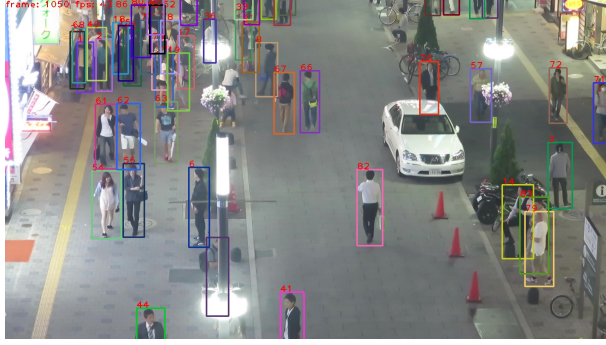
We also evaluate McByte and the baseline [40] on the MOT17 [28] validation set using the public detections provided by the dataset authors. The results are shown in Tab. 13, using the FRCNN model variant [30]. There are significant performance differences for both the baseline and McByte when using public detections, which are of lower quality compared to the private YOLOX [15] detections pre-trained on MOT17 by the baseline [40]. Public detections tend to miss more objects, leading to many false negatives.

An example comparing the quality of private and public detections is illustrated in Fig. 5. Since tracklets and their temporally propagated masks can only be initiated when a bounding box is detected, McByte’s relative performance gain over the baseline is slightly reduced when using public detections. However, even in this scenario, the temporally propagated mask-based association cue helps resolve ambiguities and improves overall tracking performance, as shown in Tab. 13.

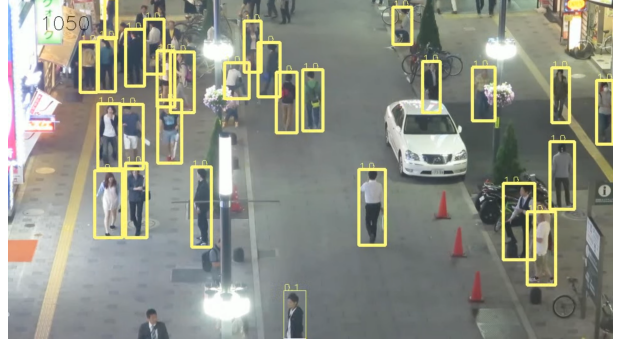
## E. McByte components more in detail

### E.1. Mask processing and management

We provide more details on mask handling introduced in Sec. 3.2 of the main paper. New objects might appear in any frame on the scene. It involves initiating new tracklets and necessitates creating new segmentation masks. We use an image segmentation model and provide the bounding boxes of new tracklets and the currently processed frame to create new masks. Further, a mask temporal propagator receives new initial masks and the frame at which they were created. Subsequently, the propagator receives the next frame, for



Private detections  
YOLOX model provided by baseline [40]



Public detections  
FRCNN model provided by MOT17 [28]

Figure 5. An example of detection quality difference. It can be seen that considerably more bounding boxes are missing in case of public detections, which negatively impacts the MOT performance. Input image data from [28], sequence MOT17-04, last frame (1050). Best seen in color.

Method	HOTA	IDF1	MOTA
MOT17 val, private detections - YOLOX [15] from baseline [40]			
Baseline	68.4	80.2	78.2
McByte	<b>69.9</b>	<b>82.8</b>	<b>78.5</b>
MOT17 val, public detections - FRCNN from [28]			
Baseline	49.0	55.3	44.5
McByte	<b>50.1</b>	<b>56.0</b>	<b>44.6</b>

Table 13. McByte and baseline [40] with private and public detections on MOT17-val

which it returns the updated mask predictions, e.g. based on the object movement and scenery change. Each tracklet has an ID and each mask included within the mask temporal propagator also gets its ID. We link masks to the tracklets based on their IDs.

Tracklets might also be marked inactive and hence removed at any frame, e.g. when a tracklet has not been matched to any detection for a long time. It induces removing the tracklets and necessitates purging the masks from the mask temporal propagator. As masks are removed from the propagator, the IDs of the remaining masks change (shift) due to the memory allocation mechanisms [6, 8]. We update the links between tracklet IDs and mask IDs to consistently keep the same masks assigned to the tracklets. Tracklet IDs are immutable. For our experimentation, we use SAM [20] as the image segmentation model and Cutie [8] as the mask temporal propagator.

The mask handling process is illustrated in Fig. 6. We process each frame of the video sequence separately. We check if there are any new initialized tracklets from the previously processed frame. If they are strongly occluded, their IDs are added to the waiting list. The tracklet posi-

tions change over the frames and they might become less occluded during the next frames. We take currently non-occluded tracklets, both newly initialized and from the waiting list, and create their masks with the image segmentation model. We include the new masks within the mask temporal propagator.

Further, we check if any tracklets have been removed at the previous frame and if so, we purge their masks from the mask temporal propagator. Regardless of adding or removing any masks, we perform mask temporal propagation to get the updated mask predictions for the current frame. The temporally propagated masks are passed to the tracker where they are used to improve the tracklet-detection association process. The process of temporally propagated masks influencing the association process is illustrated in Fig. 2 (main paper) and described in Sec. 3.3 (main paper). After the association, the tracker returns updated tracklets. Output tracklets and masks from the current frame processing constitute the input for the next frame processing. During the whole process, state of the tracklets influences the mask management, i.e. the mask creation and purging. At the same time, the masks influence the tracklet association and updating, improving the MOT performance.

## E.2. Tracklet mask visibility at the scene

In order to ensure reliable use of the temporally propagated (TP) mask, we apply several conditions, which we mention in Sec. 3.3 in the main paper. We describe them more in detail in the following subsections starting with tracklet mask visibility at the scene.

In some cases, a tracklet’s TP mask may not appear in the current frame. This can happen if the subject is completely or mostly occluded, or if the mask temporal propagator fails to predict the mask due to challenges like small visible areas, dense crowds, or poor lighting conditions. When no

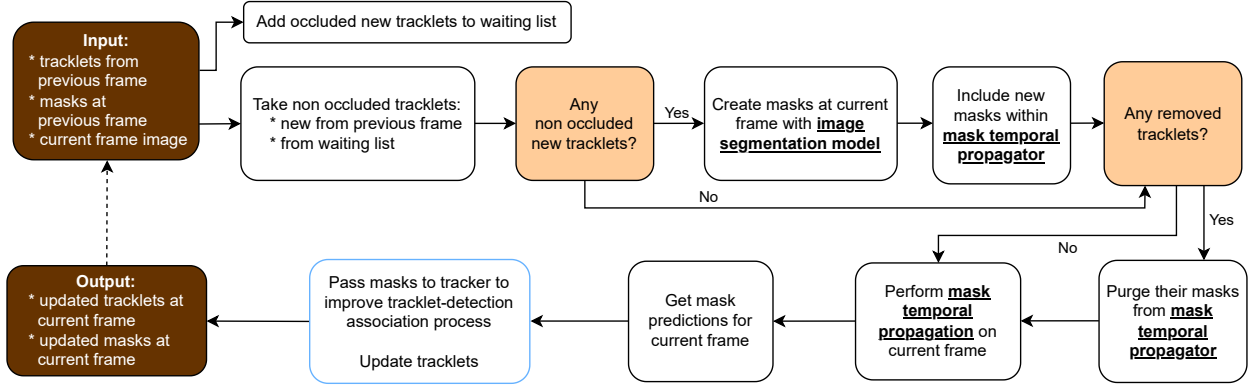


Figure 6. Diagram illustrating the mask processing and management process as described in Appendix E.1. Tracklets influence the mask management process, while masks influence the tracklet association and updating. The process of temporally propagated masks influencing the association process (the blue part) is illustrated in Fig. 2 (main paper).

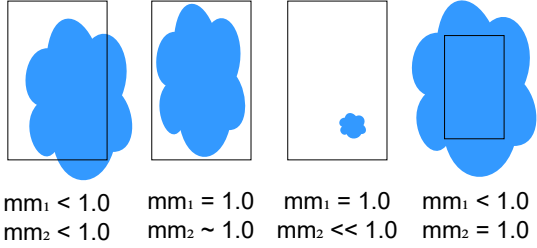


Figure 7. Cases showing the differences in  $mm_1$  and  $mm_2$  values of a temporally propagated mask (in blue) within a bounding box (Appendix E.4). The most optimal case for the mask to provide a good guidance is the second one from the left, where both  $mm_1$  and  $mm_2$  are as close to 1 as possible.

mask is predicted for a tracklet, its associations with detections are calculated using intersection over union (IoU), as done in the baseline [40].

### E.3. Mask confidence

Each predicted pixel in the mask provided by the mask temporal propagator is assigned a confidence probability [6, 8]. To determine if the TP mask prediction is reliable enough to be used in the tracklet-detection association process, we average these confidence values across all pixels for each tracklet mask separately. If the average confidence is too low, the association relies solely on the intersection over union (IoU) score.

### E.4. Bounding box coverage ( $mm_1$ ) and mask fill ratio ( $mm_2$ )

For a more detailed explanation of  $mm_1$  and  $mm_2$  (see Sec. 3.3 in the main paper), we refer to the accompanying figure that illustrates their varying values. For the reader's

convenience, this figure is also included in the supplementary material, see Fig. 7.

In the main paper, we define the bounding box coverage of the mask, referred to as  $mm_1$ . It measures the percentage of the tracklet's TP mask that falls within the detection's bounding box for each tracklet-detection pair (if the mask is visible and confident). When the entire TP mask is within the detection's bounding box, the  $mm_1$  value is 1.0, as seen in the second and third case from the left in Fig. 7. However, if part of the TP mask extends outside the bounding box, the  $mm_1$  value decreases, as shown in the first and fourth case from the left in Fig. 7. Bounding boxes can sometimes be slightly inaccurate, so we allow the  $mm_1$  value to be slightly below 1.0. However, if too much of the TP mask extends beyond the bounding box, it could indicate that the mask belongs to a different detection, in which case the mask is excluded from influencing the cost of the particular tracklet-detection pair match.

In the main paper, we also define the mask fill ratio of the bounding box, referred to as  $mm_2$ . This is calculated for each tracklet-detection pair and measures the percentage of the detection bounding box covered by the TP mask. If the TP mask only covers a small portion of the bounding box, the  $mm_2$  value will be low, as illustrated in the third case from the left in Fig. 7. This can indicate a noisy or incorrect mask prediction or that part of another TP mask is overlapping the bounding box. In our conditions (Sec. 3.3 of the main paper) we do not allow the mask to influence the tracklet-detection association in such cases.

For higher coverage, the  $mm_2$  value naturally increases. However, this value alone is not enough to confirm whether the tracklet, to which the TP mask is linked, properly matches the detection bounding box. For example, in the first case from the left in Fig. 7, the TP mask covers most of the bounding box, but it extends significantly beyond it.



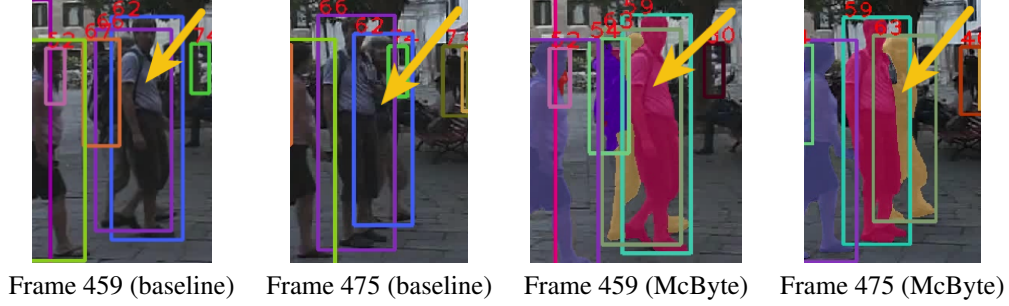


Figure 8. Visual output comparison between the baseline and McByte. With the temporally propagated mask guidance, McByte can handle the association of an ambiguous set of bounding boxes - see the subjects with IDs 59 and 63 on the output of McByte. Input image data from [28]. Best seen in color.

In the fourth case,  $mm_2$  is 1.0, indicating that the TP mask fully covers the bounding box, but it sticks out even more, making it an unlikely good match. Such situations can occur when one subject is covered by another, closer to the camera. While  $mm_2$  can approach 1.0, it is rare to see exactly 1.0 in good matches, as subjects (such as people) are not rectangular and do not fully align with their bounding boxes.

For the TP mask to have the best influence on the tracklet-detection pair match, both  $mm_1$  and  $mm_2$  should be as close to 1.0 as possible, as shown in the second case from the left in Fig. 7.

If both  $mm_1$  and  $mm_2$  meet the required conditions, the cost matrix is updated as described in the main paper (Sec. 3.3):

$$costs^{i,j} = costs^{i,j} - mm_2^{i,j} \quad (4)$$

Since high  $mm_1$  values can be misleading when a TP mask significantly extends beyond the bounding box,  $mm_1$  is used only as a gating condition to prevent poor matches (e.g., the fourth case from the left in Fig. 7). Instead, we use  $mm_2$ , which better reflects the match quality between a tracklet TP mask and a detection bounding box, provided  $mm_1$  is sufficiently high.

### E.5. Camera motion compensation

For handling camera motion, we use camera motion compensation (CMC), as outlined in Sec. 3.4 of the main paper. Our approach follows the existing methods [12, 27]. Specifically, we compute a warp (transformation) matrix that accounts for camera movement, based on extracted image features, and apply this matrix to the predicted tracklet bounding boxes. This helps adjust for the camera motion, making the tracklet predictions from the Kalman Filter [19] and the associations with detections more accurate, improving the overall tracking performance. For key-point extraction, we use the ORB (Oriented FAST and Rotated BRIEF) ap-

proach [32]. For further details, we refer the reader to the related works [12, 27].

### E.6. Additional visual example

In the main paper, we discuss that McByte can handle challenging scenarios due to the temporally propagated mask signal used in the controlled manner as an association cue (Sec. 3.3). Fig. 8 in this supplementary material illustrates our method handling association of ambiguous boxes, improving over the baseline. A figure illustrating handling long term occlusions in the crowd is placed in the main paper (Sec. 3.3).